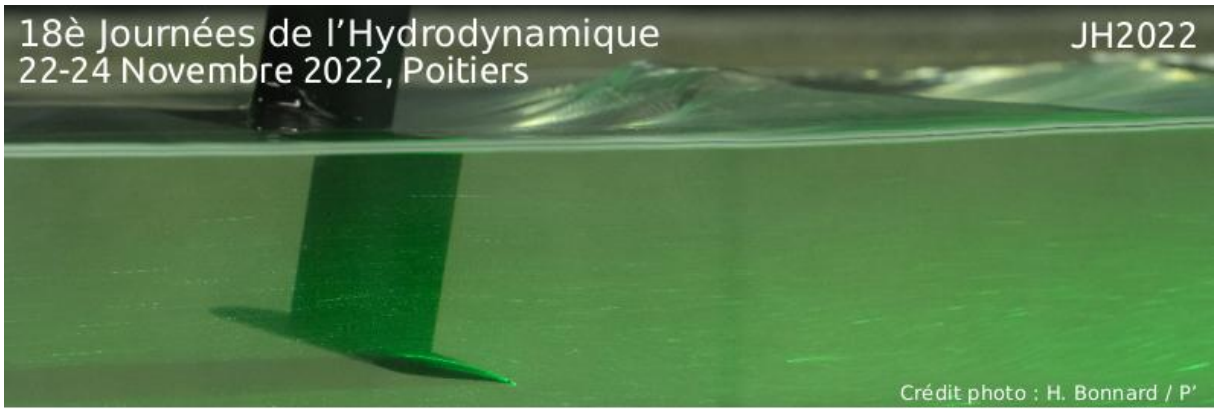


# *A LEVEL-SET APPROACH WITH EMBEDDED REINITIALIZATION*

**P. FERRO[(1),(2)], P. LANDEL[(1)], M. PESCHEUX[(1)], P. CADOT[(1)]**

*paulin.ferro@g-met.fr ; paul.landel@g-met.fr ; marc.pescheux@g-met.fr ; paul.cadot@g-met.fr*

[(1)]SARL G-MET Technologies, 424 rue de Lisbonne, La Seyne-Sur-Mer
[(2)]Corresponding author

**Résumé**

La méthode Level Set est une appoche permettant de capturer les mouvements d'interfaces entre deux fluides. Dans ce travail, une approche Level Set avec réinitialisation encapsulée est utilisée à la manière de [29] dans un contexte volumes finis au 2ème ordre. La discontinuité de la surface libre est traitée à l'aide de la Ghost Fluid Method [3]. Le solveur ségrégé est implémenté dans le code open source boite à outils OpenFOAM [31] et est testé pour plusieurs écoulements à surface libre traditionnellement rencontrés en hydrodynamique navale.

**Summary**

The Level Set method is an attractive approach for capturing interface motions between two fluids. In this work, a Level Set approach with embedded reinitialization is used in the manner of [29] for 2nd order finite volume method. The discontinuity of the free surface is handled using the Ghost Fluid Method [3]. The segregated solver is implemented in the open source CFD library OpenFOAM [31] and tested against large scale free surface flow benchmarks typically encountered in Naval hydrodynamic.

# I – Introduction

The Level Set (LS, [26])) method is a popular technique to capture interface motions between two phases. It is based on the function $\phi$, being the signed distance to the interface. The interface is thus represented by the iso-contour $\phi = 0$. In opposition to the Volume-Of-Fluid method ([11]), the interface position is readily accessible and the interface curvature is more reliable due to the smooth nature of the function $\phi$. The LS is especially interesting when used with a GFM [3]. However, the mass conservation is not guaranteed as $\phi$ is not a conserved quantity. As soon as the tangential component of the normal velocity gradient is not null, the advection step will breach the distance properties of the LS function ($|\boldsymbol{\nabla}\phi| \neq 1$) [2]. A reinitialization procedure (hyperbolic), [25], is often used to recover this LS function property and to reduce mass losses. In practice, interface displacements can occur during the reinitialization procedure leading again to mass variations. Methods have been developed to address this issue ([22], [9])), however, their implementation for arbitrary polyhedral grids is not straightforward. Other approaches can be used such as parabolic and elliptic reinitializations [1], [32]. But their use for CFD has not been evaluated and enforcing the interface location is challenging. An alternative approach is to unify both transport and reinitialization in the same equation. The variational method by energy penalization is introduced in [16] for image rendering to avoid the use of reinitalization [34]. A stabilized variational formulation is proposed in [27] and compared with [16] for benchmark test cases in a context of finite element method. Another attempt to bypass the reinitialization procedure is used in [30] for Naval applications where the LS equation is derived from the Phase-Field equation of [24]. The convective LS method is proposed in [29] where both reinitialization and transport are unified. The convective LS method has been used by [6] for gas bubble dynamics. In both [29] and [6] a sinusoidal filtering function is used to improve mass conservation in the manner of the conservative LS approach of [19]. In this work a similar approach is adopted but without the filtering function. Hence, the signed distance function is used instead of the conservative one. The present method is implemented in the 2nd order finite volume method open-source C++ code OpenFOAM [31] and tested for 4 large scale cases encountered in Naval hydrodynamic.

# II – Mathematical and numerical procedure

## II – 1 The Level-Set equation

The computational domain is composed of two subdomains $\Omega^+$ and $\Omega^-$ separated by the interface $\Gamma$. Where $\Omega^+$ and $\Omega^-$ represent respectively the domain of heavy and light phases. For a given point $\boldsymbol{x}$ the Level-Set function $\phi(x)$ is defined by the shortest distance $d$ to the interface. It is signed depending on the point owner domain to improve both numerical transport and stability near the interface by avoiding $\boldsymbol{\nabla}\phi$ discontinuities (equation 1).

$$\phi(\boldsymbol{x}) = \begin{cases} 0 & \boldsymbol{x} \in \Gamma \\ d(\boldsymbol{x}) & \boldsymbol{x} \in \Omega^+ \\ -d(\boldsymbol{x}) & \boldsymbol{x} \in \Omega^- \end{cases} \tag{1}$$

Consequently to this definition (eq 1), $\forall x, |\boldsymbol{\nabla}\phi| = 1$. Interface normal $\boldsymbol{n}$ and curvature $\kappa$ can be computed as follow:

$$\boldsymbol{n} = \frac{\boldsymbol{\nabla}\phi}{|\boldsymbol{\nabla}\phi|} \tag{2}$$

$$\kappa = \boldsymbol{\nabla} \cdot \boldsymbol{n} \tag{3}$$

The Level-Set function $\phi$ is advected in a flow field $\boldsymbol{u}$ (assumed incompressible) using a transport equation:

$$\frac{\partial \phi}{\partial t} + \boldsymbol{\nabla} \cdot (\boldsymbol{u}\phi) = 0 \tag{4}$$

The transport of the Level-Set function will breach the distance property and cause mass variations. To limit such consequences, a reinitialization procedure is generally adopted by solving the following Hamilton-Jacobi problem, [26]:

$$\frac{\partial \phi}{\partial \tau} = S(\phi_0)(1 - |\boldsymbol{\nabla}\phi|) \tag{5}$$

Where $S$ is the sign function, $\phi_0$ the initial value of the signed distance function and $\tau$ has the dimension of a length. As indicated above solving the reinitialization equation can significantly shift the interface. For structured grids the sub-cell fix method has been proposed in [22] to limit such a behavior and improved later, in [10]. As in [29] we define the penality factor $\lambda$ such as :

$$\frac{\partial \phi}{\partial t} = \lambda \frac{\partial \phi}{\partial \tau} \tag{6}$$

resulting in:

$$\frac{\partial \phi}{\partial t} + \boldsymbol{\nabla} \cdot (\boldsymbol{u}\phi) + \lambda S(\phi_0)(|\boldsymbol{\nabla}\phi| - 1) = 0 \tag{7}$$

By defining $\boldsymbol{w} = \lambda S(\phi_0)\boldsymbol{n}$ [25], equation 7 can be written in a conservative way allowing finite volume implicit discretization:

$$\frac{\partial \phi}{\partial t} + \boldsymbol{\nabla} \cdot (\boldsymbol{u}\phi) + \boldsymbol{\nabla} \cdot (\phi \boldsymbol{w}) - \phi \boldsymbol{\nabla} \cdot \boldsymbol{w} = \lambda S(\phi_0) \tag{8}$$

In this equation (8), the reinitialization is embedded during the transport. $S(\phi_0)$ is smoothed to improve the numerical stability near the interface :

$$S(\phi_0) = \frac{\phi_0}{\sqrt{\phi_0^2 + \epsilon^2}} \tag{9}$$

Where $\epsilon$ is chosen as 2 or 3 times a reference cell size. In this study, time derivative is discretized with first order Euler or 2nd order backward schemes. For the LHS, the convective terms $\boldsymbol{\nabla} \cdot (\phi \boldsymbol{w})$ and $\boldsymbol{\nabla} \cdot (\boldsymbol{u}\phi)$ are discretized using 2nd order TVD MUSCL scheme [28] and the last term is treated implicitly. The penalty coefficient $\lambda$ which has the dimension of a velocity is defined as :

$$\lambda = min(\sigma \frac{\Delta x}{\Delta t}, 1.0) \tag{10}$$

With $\Delta x$ being the local mesh size for dealing with unstructured and complex meshes and $\Delta t$ the time step. $\sigma$ is usually taken as 0.5. The Level-Set function is used to compute the phase fraction $\alpha$ using a filtering function:

$$\alpha = \frac{1}{2}\left(tanh\left(\frac{\pi\phi}{\epsilon}\right) + 1\right) \tag{11}$$

$\alpha$ is then used to calculate the mixture viscosity $\mu$ as:

$$\mu = \alpha\mu^{+} + (1-\alpha)\,\mu^{-} \tag{12}$$

The sharp density field is enforced in a consistent manner with the GFM.

$$\begin{cases} \rho = \rho^{+} & if\ \phi > 0 \\ \rho = \rho^{-} & if\ \phi < 0 \end{cases} \tag{13}$$

$\mu^{+}$ and $\mu^{-}$ are the dynamic viscosity of heavy and light phases and $\rho^{+}$ and $\rho^{-}$ their density.

## II – 2 Pressure-velocity formulation

In the context of large scale flows, surface force can be neglected. Hence, the momentum equation in each phase can be written as follow:

$$\begin{gathered} \frac{\partial \boldsymbol{u}}{\partial t} + \boldsymbol{\nabla}\cdot(\boldsymbol{u}\cdot\boldsymbol{u}) = \frac{1}{\rho}(-\boldsymbol{\nabla}p + \\ \rho\boldsymbol{g} + \boldsymbol{\nabla^2}(\mu_{eff}\boldsymbol{u}) + \boldsymbol{\nabla u}\cdot\boldsymbol{\nabla}(\mu_{eff})) \end{gathered} \tag{14}$$

Where $\mu_{eff}$ is the effective viscosity. The momentum equations is formulated in term of piezometric pressure $p_d$, [21]:

$$p = p_d + \rho\boldsymbol{g}\cdot\boldsymbol{x} \tag{15}$$

The incompressible continuity equation is

$$\boldsymbol{\nabla}\cdot\boldsymbol{u} = 0 \tag{16}$$

Assuming a piece-wise density field, equation 14 takes the following form in each phase domain $\Omega^{+}$ and $\Omega^{-}$ :

$$\begin{gathered} \frac{\partial \boldsymbol{u}}{\partial t} + \boldsymbol{\nabla}\cdot(\boldsymbol{u}\cdot\boldsymbol{u}) = \frac{1}{\rho}(\boldsymbol{\nabla}p_d + \\ \boldsymbol{\nabla^2}(\mu_{eff}\boldsymbol{u}) + \boldsymbol{\nabla u}\cdot\boldsymbol{\nabla}(\mu_{eff})),\ in\ \Omega^{+}\ or\ \Omega^{-} \end{gathered} \tag{17}$$

With continuous velocity and dynamic viscosity fields, equation 17 is completed by the following set of jump conditions at the interface $\Gamma$:

$$\left[\frac{\boldsymbol{\nabla}p_d}{\rho}\right]_{\Gamma} = 0 \tag{18}$$

$$[p_d]_{\Gamma} = [\rho]_{\Gamma}\,\boldsymbol{g}\cdot\boldsymbol{x}_{\Gamma} = \mathcal{H} \tag{19}$$

Where $\boldsymbol{x}_{\Gamma}$ is the interface coordinate vector. The bracket notation $[.]_{\Gamma}$ indicates a jump value between both sides of the interface. The jump conditions are used to modify the discretization operators at interface following the Ghost Fluid Method, [3]). The

reader is referred to [30], [8] or [4] for the detailed modification of Laplacian and gradient operators. The momentum equation 17 is discretized in the following manner.

$$a_C \boldsymbol{u}_C + \sum_N a_N \boldsymbol{u}_N = \boldsymbol{b}_C(\boldsymbol{u}) \tag{20}$$

Where $a_c$ are the diagonal coefficients and $a_N$ the off diagonal ones of the momentum equation. The source term $b_b$ includes all the explicit contributions (old time pressure gradient, non-orthogonality correction...). Then following [31], the pressure Poisson equation is obtained using the continuity equation 16 as follows:

$$\boldsymbol{\nabla} \cdot \left( \frac{1}{a_c} \frac{\boldsymbol{\nabla} p_d}{\rho} \right) = \boldsymbol{\nabla} \cdot \boldsymbol{u}_C \tag{21}$$

The pressure gradient is separated into orthogonal and non-orthogonal contributions following the over-relaxed approach [14]. The orthogonal part is treated implicitly while the latest is calculated explicitly. After solving the pressure Poisson equation velocity field and flux are updated.

### II – 3 Solver chart

The LS with embedded reinitialization equation, the momentum and the pressure Poisson equations are solved in a segregated manner with the PIMPLE algorithm available in OpenFOAM. The PIMPLE algorithm is a combination of SIMPLE ([20]) and PISO ([20, 12]) algorithms. At the beginning of time step, the SIMPLE loop starts. Grid and flux are updated knowing mesh motions and the Level Set equation is solved (8). The pressure Poisson equation is solved iteratively within the PISO loop and finally turbulence equations are solved. The procedure is summarized in the following algorithm 1.

```
1  while t < t_end do:
2
3      Call dynamic mesh motion
4      Update grid and flux
5      Solve Level-Set equation 8
6      Update jump conditions 18 and 19
7
8      do PIMPLE loop:
9
10         Build u equation 20
11         Optionaly solve u equation 20
12
13         do PISO:
14
15             Solve Pressure Poisson equation 21
16             Update flux and velocity
17
18 Solve turbulence equations
```

Listing 1: Segregated flow algorithm

# III – Test cases

## III – 1 Partial Dam break failure, [5]

A three dimentional partial dam break flow has been simulated. The result are compared with the experiment data of [5]. This test case have also been studied by [7]. It consists in simulating the flow of a 0.6 m high, 1 m long and 2 m width water column into a vertical 1 m width breach. The geometry is illustrated in Figure 1. The structured mesh is composed of 5 M cells. An adjustable time step has been used with a maximum Courant number of 0.5. Turbulence effects are calculated with the k-omega SST model, [17]. The water elevation has been calculated and compared to the experimental data measurements at two probe positions illustrated Figure 1. The Figure 2 represents the surface elevation evolution and their comparison with experimental data for the two probes. The results are in excellent agreement with experimental data. Finally, Figure 3 illustrates the free surface contour $\phi = 0$ at time 0.25, 0.5 and 0.75 s.

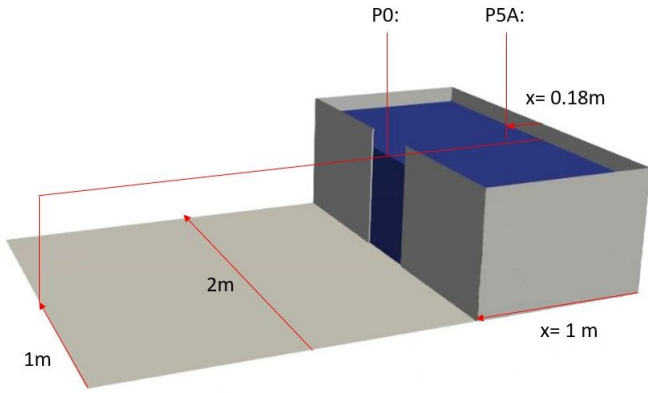


Figure 1: Partial Dam break geometry

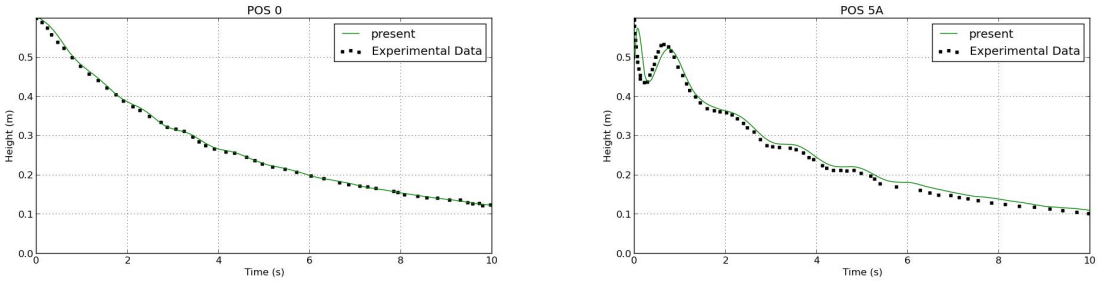


Figure 2: Water elevation at at probes P0 and P5A

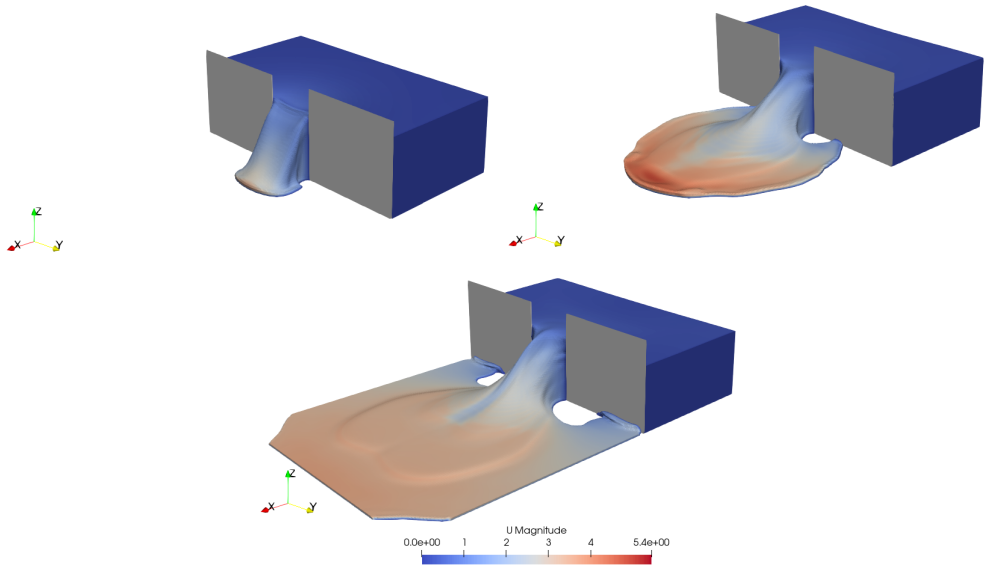


Figure 3: partial dam break flow illustrations

| Property | Wedge | Bow flare |
|---|---|---|
| Breadth [m] | 0.5 | 032 |
| Vertical distance from keel to knuckle [m] | 0.29 | 0.203 |
| Length of measuring section [m] | 0.2 | 0.1 |
| Length of each dummy section [m] | 0.4 | 0.45 |
| Total length [m] | 1.00 | 1.00 |
| Weight of drop rig (without ballast) [kg] | 141 | 161 |
| Ballast weight [kg] | 100 | 100 |
| Total weight of rig [kg] | 241 | 261 |
| Weight of measuring section [kg] | 14.5 | 6.9 |

Table 1: Wedge and Bow flare section. Main data

### III – 2 Water entry test cases, [35]

In this section the wedge and bow flare test cases from [35] are reproduced with a 2D assumption and a symmetry plane. The main properties for both test sections are summarized in table 1. The slamming force and velocity are compared with the experimental data and numerical results of [35], [33] and [23]. The structured meshes are generated with blockMesh, composed of 40 k cells and illustrated Figure 4. Maximal non-orthogonality grid is 59° for wedge case and 78° for bow flare case. An adjustable time step has been used with a maximum Courant number of 0.5. Turbulence effects are calculated with the k-omega SST model, [17]. Spatial and temporal derivatives are discretized with 2nd order schemes (2nd order upwind and backward). The body motion is computed using a 6 DoF module where a non deforming grid strategy is adopted. Results are presented for slamming force and velocity on Figure 5. The overall trends are well captured although some discrepancies are observed, especially for maximal slamming force that could be explained by the 2D assumption. The free surface and water jets are illustrated on Figure 6 at two times : peak force and latest times.

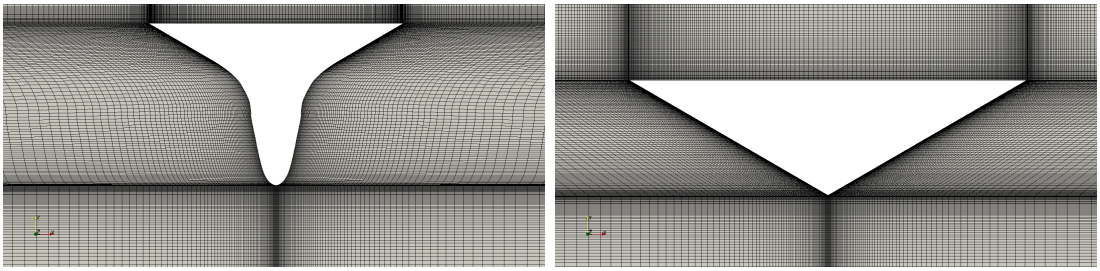

Figure 4: Structured blockMesh grids for wedge and bow flare cases

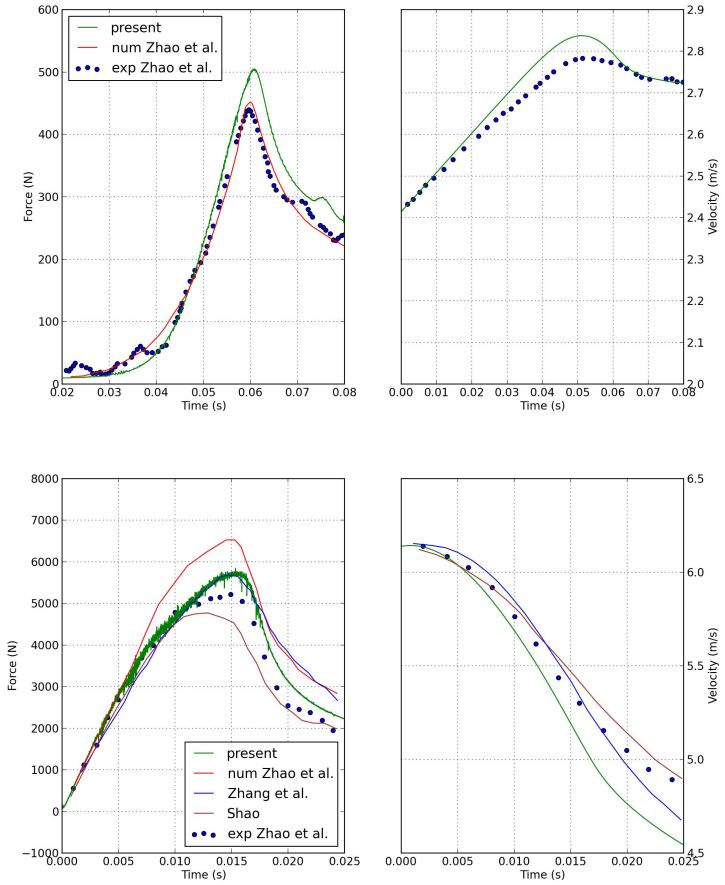


Figure 5: Slamming forces and velocities for wedge and bow flare cases. Top : bow flare. Bottom : wedge

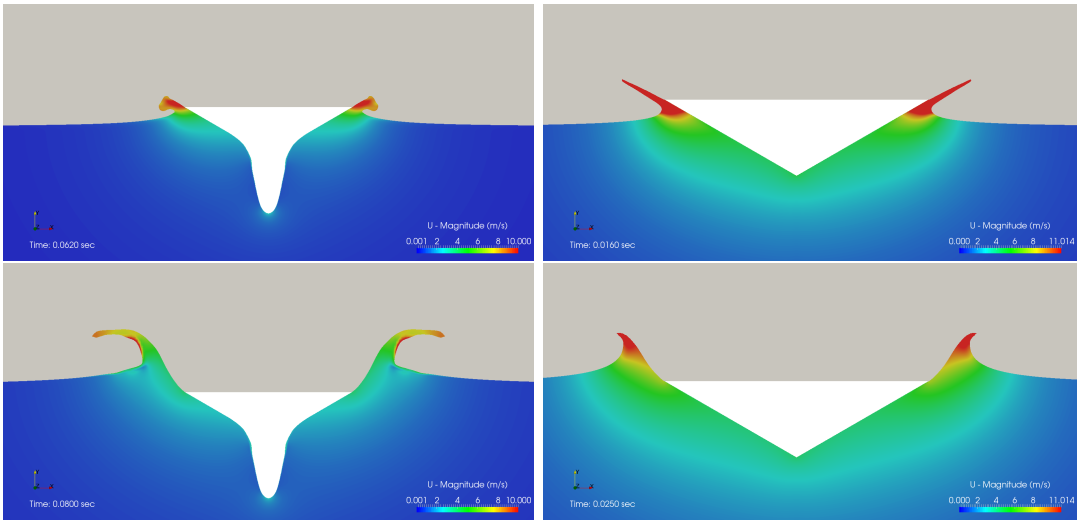


Figure 6: Free surface evolution colored by velocity magnitude. Left : bow flare. Right : wedge

### III – 3 Periodic wave propagation, [15]

The 2D periodic domain wave propagation exercise is a numerical test case popularized in [15]. It consists in propagating a wave in 2D domain of length 3.79 m and height 0.8 m. A stream function of height H = 0.125 m and period T = 2 s is initialized with the package waves2Foam, [13]. The mean water level is 0.4 m above the floor. The structured grid is composed of 379x80 cells. Following table 1 of [15], the settings used in fvSchemes and fvSolution are the same than in the dambreak tutorial. The results are compared with the one obtained with interFoam solver in Figure 7. The present approach with embedded reinitialization successfully allows to maintain the wave height, Figure 8, showing that mass conservation is well preserved for long time simulations and that spurious air velocities do not occur thanks to the GFM. On the other side the light phase accelerations (clearly visible on Figure 8) near the free surface explain the behavior obtained with interFoam. As explained by [15], these light phase accelerations are caused by the unbalances between dynamic pressure gradient and density gradient in the vicinity of the free surface. The time step being controlled by the Courant number, light phase accelerations cause a drastic limitation of the time step with interFoam. Its order of magnitude is 3 ms with interFoam, whereas it is 12 ms with the present approach.

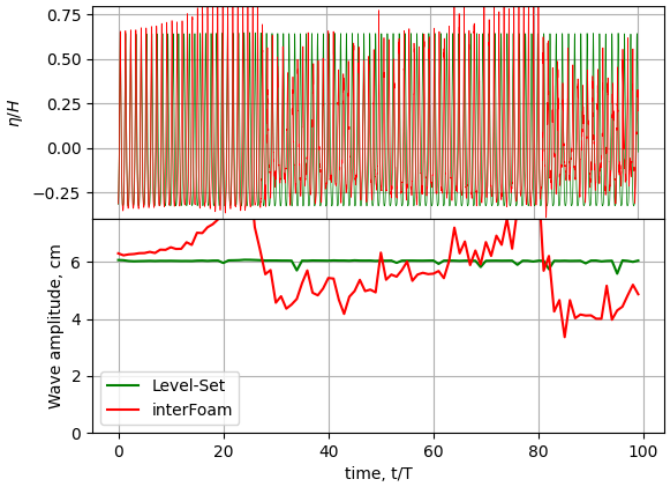


Figure 7: Adimentionalized surface elevation $\eta/H$ and wave amplitude (cm). Comparison between present approach (green) and interFoam solver (red)

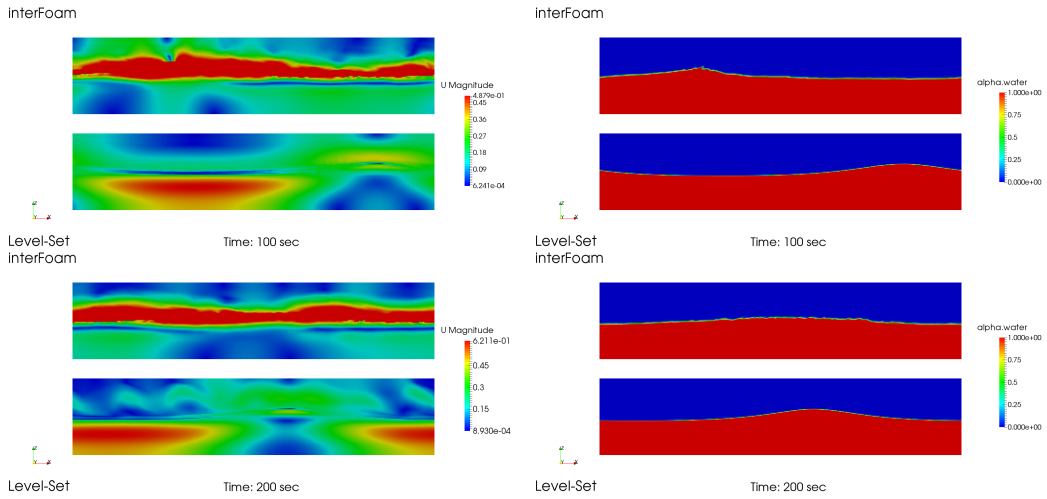


Figure 8: Wave velocity and volume fraction at two different snapshot (left: 50T and right 100T)

### III – 4 DTMB 5415 ship resistance, [18]

The DTMB 5415, [18], is a model scale ship with scale factor of 24.824. Main particulars are detailed in Table 2. The experiment of [18] consists in simulating a towing tank test at different Froude numbers with 2 degree of freedom (trim and sinkage). The resistance, motions and wave pattern are measured and used as reference data for comparison with numerical results. Simulations are carried out in the fixed ship reference frame with a symmetry hypothesis on the y = 0 plane. The air/water flow is imposed at the entrance of the computational box. A pressure reference is imposed on top through atmospheric boundary conditions. For bottom and lateral patches, a slip condition is used, while, for outlet ones, zero gradient conditions are defined. Wall functions are used for the hull patch. The computational grid is generated with snappyHexMesh, is composed of 2.0 M cells and is illustrated figures 9. Cells are refined close to the free surface. Refinement boxes are defined in the near-hull region whereas coarse cells are used for the far-field

| | Main particulars (Full Scale) | Main particulars (model Scale) |
|---|---|---|
| Lpp(m) | 142 | 5.72 |
| Draft (m) | 6.15 | 0.248 |
| Displacement (m3) | 8424.4 | 0.55 |
| Wetted area ($m^2$) | 2972.6 | 4.823 |
| LCB (%Lpp) | -0.683 | -0.683 |
| VCG (m) | 7.5473 | 0.304 |

Table 2: DTMB 5415. Main particulars

region. The time step is fixed at 10 ms for all Froude numbers. The pressure velocity coupling is achieved using 3 PIMPLE and 3 PISO loops. The Figure 12 represents the trim angles, sinkage displacements and force coefficients calculated and their comparison with experimental data for the different Froude numbers. The calculation results are in good agreement with experimental data. The free surface elevations (z/Lpp) are compared at a Froude number of 0.28 (Figure 13) and for four positions: the hull and three longitudinal cut planes. The first plane is located at y/Lpp= 0.082, the second one at y/Lpp= 0.172 and the last one at y/Lpp= 0.301. The trend is properly calculated especially for the three first ones. The global wake pattern is also compared with the experimental data of [18] on figure 11. The Figure 10 shows the sharp dynamic pressure field given by the Ghost Fluid Method and the volume fraction field.

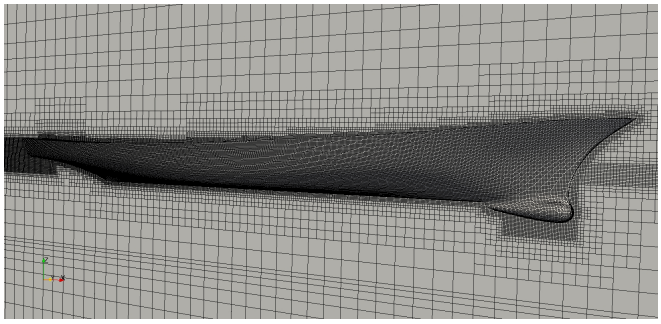

Figure 9: Unstructured mesh generated with snappyHexMesh

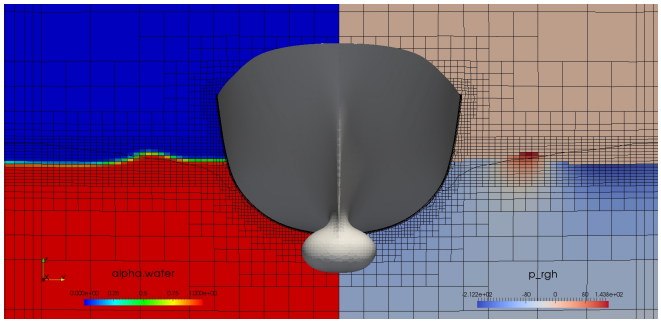


Figure 10: Phase fraction and dynamic pressure at x = 3.5 m

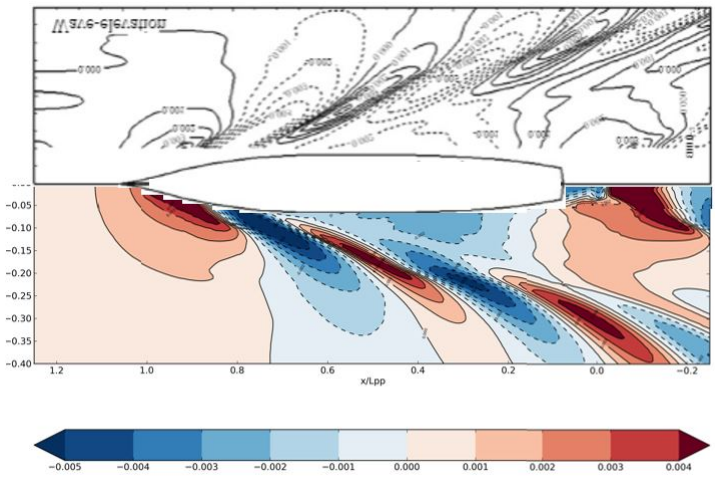


Figure 11: Surface Elevation contours ($\Delta z/L_{pp} = 0.001$)
- top : experimental measurements - bot : LSFoam

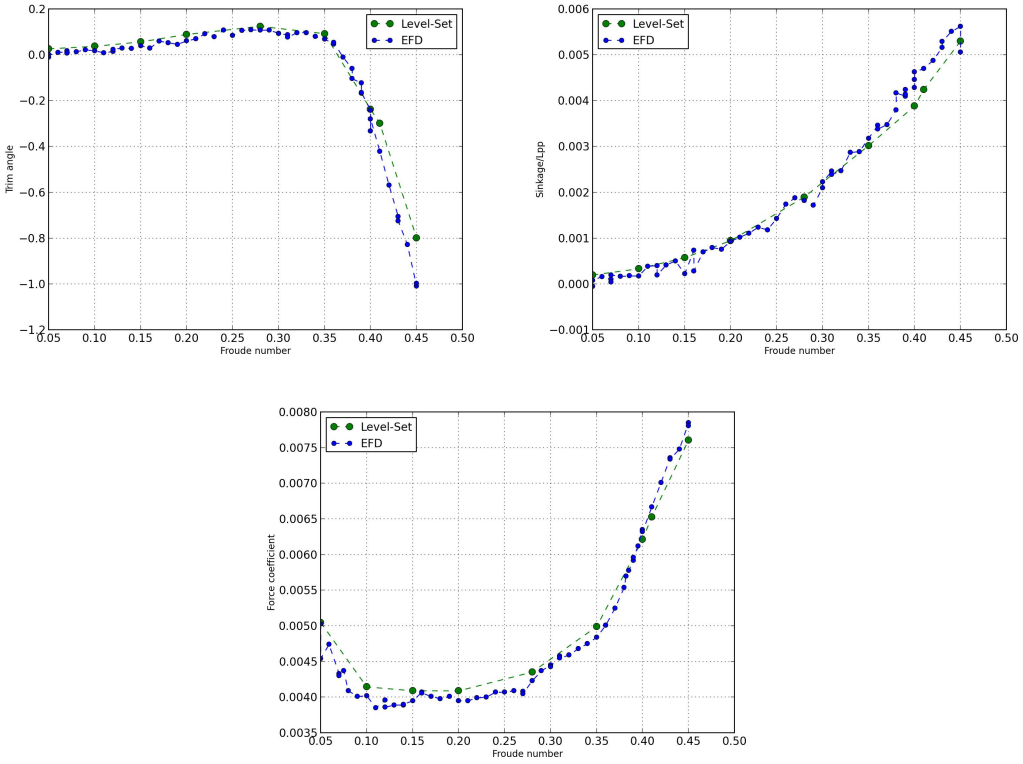


Figure 12: Trim, Sinkage and force coefficient results and comparisons for different Froude numbers

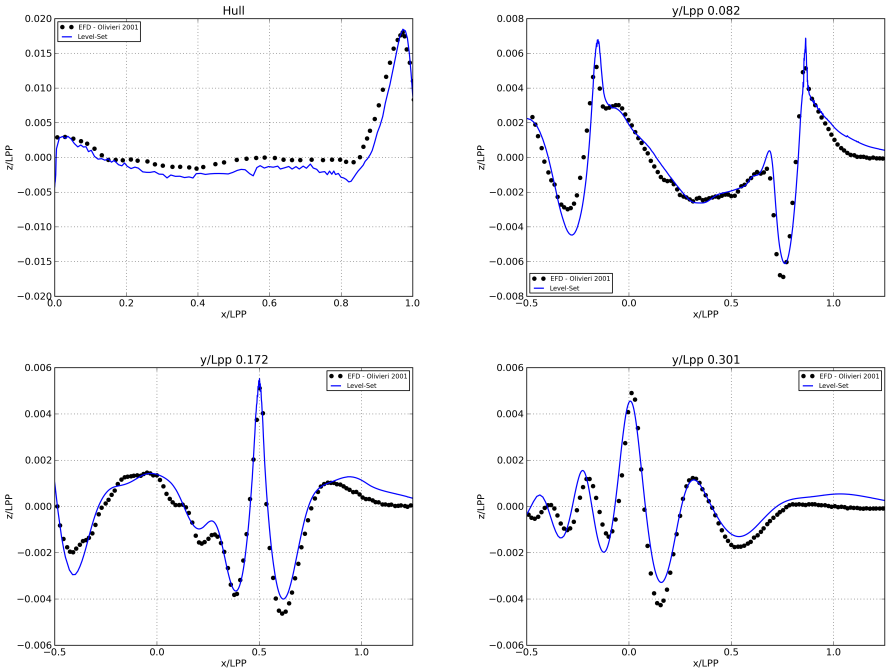


Figure 13: Adimentionalized free surface elevation comparisons at a Froude number of 0.28

## IV – Conclusions

In this study, a Level-Set/GFM solver using OpenFOAM has been presented. The present approach uses a Level-Set equation with embedded reinitialization for overcoming the main drawback of the standard Hamilton-Jacobi problem. The idea of [29] has been used as a basis but without filtering function and with a suitable form for implicit FVM. The penalty factor uses a local cell size formulation for dealing with complex non-uniform grids. The flow solver takes advantages of the PIMPLE algorithm available in OpenFOAM. The discretization operators are modified near the interface to take into account the density discontinuity through the GFM. The present solver is tested against 4 test cases with moderate free surface deformations. The overall results are in good agreement with the experimental data. Despite the choice of a Level-Set approach, mass conservation is well preserved especially considering the uses of 2nd order discretization schemes. The present approach seems very promising for wave propagation simulations. Future works considering sea-keeping analysis or more complex free surface motions should be conducted.

## References

[1] K. D. Basting, C. A minimization-based finite element formulation for interface-preserving level set reinitialization. *Computing*, 95:13–25, 2013.

[2] F. Couderc. *Développement d'un code de calcul pour la simulation d'écoulements de fluides non miscibles. Application à la désintégration assistée d'un jet liquide par un courant gazeux.* Theses, Ecole nationale superieure de l'aeronautique et de l'espace, Feb. 2007.

[3] R. P. Fedkiw, T. Aslam, and S. Xu. The ghost fluid method for deflagration and detonation discontinuities. *Journal of Computational Physics*, 154(2), 9 1999.

[4] P. Ferro, P. Landel, M. Pescheux, and S. Guillot. Development of a free surface flow solver using the ghost fluid method on openfoam. *Ocean Engineering*, 253:111236, 2022.

[5] L. Fraccarollo and E. F. Toro. Experimental and numerical assessment of the shallow water model for two-dimensional dam-break type problems. *Journal of Hydraulic Research*, 33(6):843–864, 1995.

[6] M. Grave, J. J. Camata, and A. L. Coutinho. A new convected level-set method for gas bubble dynamics. *Computers and Fluids*, 209:104667, 2020.

[7] Z. Gu, H. Wen, C. Yu, and T. W. Sheu. Interface-preserving level set method for simulating dam-break flows. *Journal of Computational Physics*, 374:249–280, 2018.

[8] M. Haghshenas, J. A. Wilson, and R. Kumar. Finite volume ghost fluid method implementation of interfacial forces in piso loop. *Journal of Computational Physics*, 376:20–27, 2019.

[9] D. Hartmann, M. Meinke, and W. Schröder. The constrained reinitialization equation for level set methods. *Journal of Computational Physics*, 229(5):1514–1535, 2010.

[10] D. Hartmann, M. Meinke, and W. Schröder. Differential equation based constrained reinitialization for level set methods. *J. Comput. Phys.*, 227:6821–6845, 2008.

[11] C. Hirt and B. Nichols. Volume of fluid (vof) method for the dynamics of free boundaries. *Journal of Computational Physics*, 39(1):201–225, 1981.

[12] R. Issa. Solution of the implicitly discretised fluid flow equations by operator-splitting. *Journal of Computational Physics*, 62(1):40–65, 1986.

[13] N. G. Jacobsen, D. R. Fuhrman, and J. Fredsøe. A wave generation toolbox for the open-source cfd library: Openfoam®. *International Journal for Numerical Methods in Fluids*, 70(9):1073–1088, 2012.

[14] H. Jasak. *Error Analysis and Estimation for the Finite Volume Method with Applications to Fluid Flows*. PhD thesis, 1996.

[15] B. E. Larsen, D. R. Fuhrman, and J. Roenby. Performance of interfoam on the simulation of progressive waves. *Coastal Engineering Journal*, 61(3):380–400, 2019.

[16] C. Li, C. Xu, C. Gui, and M. D. Fox. Distance regularized level set evolution and its application to image segmentation. *IEEE Transactions on Image Processing*, 19(12):3243–3254, 2010.

[17] F. R. Menter, M. Kuntz, R. Langtry, K. Hanjalic, Y. Nagano, and M. J. Tummers. Ten years of industrial experience with the sst turbulence model, 4th:; internal symposium, turbulence, heat and mass transfer. In *TURBULENCE HEAT AND MASS TRANSFER, Turbulence, heat and mass transfer, 4th:; Internal Symposium, Turbulence, heat and mass transfer*, volume 4, pages 625–632, New York, 2003. Begell House,;.

[18] A. Olivieri, F. Pistani, A. Avanzini, F. Stern, and R. Penna. Towing tank experiments of resistance, sinkage and trim, boundary layer, wake, and free surface flow around a naval combatant insean 2340 model. 2001.

[19] E. Olsson, G. Kreiss, and S. Zahedi. A conservative level set method for two phase flow ii. *Journal of Computational Physics*, 225(1):785–807, 2007.

[20] S. Patankar and D. Spalding. A calculation procedure for heat, mass and momentum transfer in three-dimensional parabolic flows. *International Journal of Heat and Mass Transfer*, 15(10):1787–1806, 1972.

[21] H. Rusche. *Computational Fluid Dynamics of Dispersed Two-Phase Flows at High Phase Fractions*. PhD thesis, Imperial College, London, 2002.

[22] G. Russo and P. Smereka. A remark on computing distance functions. *Journal of Computational Physics*, 163(1):51–67, 2000.

[23] S. Shao. Incompressible sph simulation of water entry of a free-falling object. *International Journal for Numerical Methods in Fluids*, 59(1):91–115, 2009.

[24] Y. Sun and C. Beckermann. A two-phase diffuse-interface model for hele–shaw flows with large property contrasts. *Physica D: Nonlinear Phenomena*, 237(23):3089–3098, 2008.

[25] M. Sussman, E. Fatemi, P. Smereka, and S. Osher. An improved level set method for incompressible two-phase flows. *Computers and Fluids*, 27(5):663–680, 1998.

[26] M. Sussman, P. Smereka, and S. Osher. A level set approach for computing solutions to incompressible two-phase flow. *Journal of Computational Physics*, 114(1):146–159, 1994.

[27] M. K. Touré and A. Soulaïmani. Stabilized finite element methods for solving the level set equation without reinitialization. *Computers and Mathematics with Applications*, 71(8):1602–1623, 2016.

[28] B. van Leer. Towards the ultimate conservative difference scheme. v. a second-order sequel to godunov's method. *Journal of Computational Physics*, 32(1):101–136, 1979.

[29] Ville, S. Luisa, and C. Thierry. Convected level set method for the numerical simulation of fluid buckling. *International Journal for Numerical Methods in Fluids*, 66(3):324–344, 2011.

[30] V. Vukcevic. *Numerical Modelling of Coupled Potential and Viscous Flow for Marine Applications*. PhD thesis, 11 2016.

[31] H. G. Weller, G. Tabor, H. Jasak, and C. Fureby. A tensorial approach to computational continuum mechanics using object-oriented techniques. *Computers in Physics*, 12(6):620–631, 1998.

[32] T. Xue, W. Sun, S. Adriaenssens, Y. Wei, and C. Liu. A new finite element level set reinitialization method based on the shifted boundary method. *Journal of Computational Physics*, 438:110360, 2021.

[33] D. G. D. R. A. H.-R. D. G. P. J. X. L. Yali Zhang, Qingping Zou. A level set immersed boundary method for water entry and exit. *Communications in Computational Physics*, 8(2):265–288, 2010.

[34] K. Zhang, L. Zhang, H. Song, and D. Zhang. Reinitialization Free Level Set Evolution via Reaction Diffusion. *IEEE Transactions on Image Processing*, 22(1):258–271, 2013.

[35] R. Zhao, O. M. Faltinsen, and J. V. Aarsnes. Water entry of arbitrary two-dimensional sections with and without flow separation. 1996.